ISSN (e): 2250 – 3005 || Volume, 07 || Issue, 11|| November – 2017 ||
International Journal of Computational Engineering Research (IJCER)

Effect of Position of Wall Mounted Surface Protrusion in Drag Characteristics At Low Reynolds Number

Raj Narayan Gopalakrishnan [1,] Peter J. Disimile [2]
[1,2]*Department of Aerospace Engineering, University of Cincinnati, Cincinnati, OH, USA*
Corresponding Author: Raj Narayan Gopalakrishan

ABSTRACT
The drag characteristics of different combinations of cubical surface protrusions were studied using computational analysis tools in order to better understand the drag physics. Initially, the results from a flat plate simulation was validated with experimental results to ensure that the computational solutions obtained were reliable. Following the validation study, geometric features of the simulation domain was modified to establish its effect in drag values. This provided insight into the effect of the wall of water tunnel on the drag characteristics. Once a baseline setup was arrived at, surface protrusions were added onto the top surface of the flat plate and the drag characteristics studied. It was found that the addition of a single cubical protrusion of frontal area of $1cm^2$ at low Reynolds number increased the drag by approximately 10%. Surface protrusions were later added in the row-wise and column-wise configurations to establish its effect on drag values.

Keywords: CFD analysis, Low Reynolds number, Wall mounted Cubes, Drag Coefficient, Laminar flow, Inline and Staggered

---

Date of Submission: 27-09-2017 Date of acceptance: 08-12-2017

I. INTRODUCTION

Based on the freestream velocity, the flow over a flat plate can be classified as either laminar, transitional or turbulent. Laminar flow is usually associated with streamlined flow with a lower drag loss. Any disturbances or perturbations to the freestream can trip the flow into a transitional state and then into turbulent condition, thereby increasing drag losses. Hence, it's ideal to maintain the flow as laminar as long as possible to ensure that the flow losses due to drag is minimized. But this is not always possible in practical scenario. Surface imperfections can have calamitic effect on the laminar boundary layer, transitioning the flow into a turbulent regime. The current study is intended to establish the effect of such surface protrusion by calculating drag values for laminar scenario.

Significant research has been done in the field of wall mounted protrusion in laminar and turbulent flow. The majority of the study has concentrated on heat transfer and location of separation point as the topic of interest. The seminal work done by Meinders and Hanjalic [1], [2] and [3] concentrated on the heat transfer from wall-mounted cubes, in different spacial configurations, both inline and staggered. In [1], they observed that a large non-uniformity existed in convective heat transfer distribution due to the complex structure of vortices formed due to the interaction of flow with the surface protrusions. They established that a region of flow reattachment exhibited high convective heat transfer while region of flow separation had comparatively lower convective heat transfer. Additionally, they observed strong gradient in convective heat transfer along the first set of cubes, with the first cube having the lowest convective heat transfer factor, and 3rd cube seeing the establishment of fully developed thermal boundary layer. From their study [2], they concluded that major differences existed in terms of local heat transfer coefficient for inline and staggered configuration. But this did not affect the cube-averaged heat transfer coefficient value, implying that the bulk flow was the decisive parameter that affects the heat transfer coefficient. They also established that there was no major Reynolds number dependence in cube-averaged heat transfer coefficient for the Reynolds number considered in their study [3]. The combination of these three studies provides us with a significant understanding of the flow physics as it relates to the heat transfer parameter in the presence of a surface protrusion.

Nakamura et al. [4] extended on the work done by Meinders and Hanjalic and explored the effect of higher Reynolds number on heat transfer coefficient. From their study, they concluded that the Nusselt number data showed similar trend as to the values observed by Meinders and Hanjalic. They also observed high values of

heat transfer coefficient in the region associated with the horse-shoe vortex, primarily in front and sides of the first cube. The work done by Heidarzadeh et al. [5], who used Large Eddy Simulation (LES) model to study the flow over wall mounted cubes, obtained the same result; thereby proving that computational tools are capable of accurate prediction of the thermal physics associated with such flows.
Schmidt and Thiele [6] studied the impact of computational method used in the accurate prediction of flow physics. They studied Large Eddy Simulation (LES), Detached Eddy Simulation (DES) and unsteady RANS simulation for wall mounted cubes and established that in order to accurately capture the flow physics, refined mesh resolution was required for both LES and DES models. In case of wall mounted cylinders, they observed that coarse mesh resolution did not significantly affect the mean velocity data. This indicates that the flow over wall mounted protrusions can be studied using DES models (which are computationally less expensive than LES models), but the mesh criterion based on geometry must be taken into consideration. Also, they note that LES models perform superior to RANS models in cases with high amount of unsteady motion, which is common in cases with wall mounted surface protrusions.

Hong et al. [7] studied the laminar separation and reattachment of the flow over wall mounted protrusions. They used computational tools to study the effect of Reynolds number, aspect ratio of protrusion and initial boundary layer thickness on the flow field. They concluded that increase in Reynolds number led to the increase in size of separation region, leading to separation flow gaining strength. Also, the presence of larger boundary layer thickness leads to an increase in size of separation region, but reduction in the strength of separation flow. This study provides us with insight of placement of surface protrusion in the stream-wise direction, and quantitatively expresses this in terms of separation region size.
Eslami et al. [8] has studied the laminar flow over wall mounted cubes of various surface configurations. They have shown that there is a direct correlation between the spacing between the cubes and Reynolds number with the vortical structure formed around the cubes. For inline configuration with the spacing between cubes smaller than 3.5 times the cube length, one single horseshoe vortex was observed to warp the space between the cubes. If this spacing was increased beyond 3.5, the single horseshoe vortex was seen to split into two, attaching to the walls of the cubes. For staggered configuration, the flow field was observed to be completely asymmetric and was highly dependent on locations of the cubes. Also, they observed that when stream-wise and lateral spacings were kept equal, usual recirculation patterns were not observed. Instead a significant wake region was observed closer to the lateral wall of the second cube (on the side adjacent to the first cube). These studies establish the complex nature of 3D vortical structures that evolve from the flow interaction with surface protrusions.

II. COMPUTATIONAL METHODOLOGY

For the current study, 5 different geometric packing arrangements (cases) were generated; a validation case, a baseline case, case with 1 cube, case with 4 cubes in row formation and case with 4 cubes in column formation. All these geometries were generated using commercial CAD software, SolidWorks; and meshed using ICEM-CFD. The individual geometries are shown in figures in Table 1. Commercial CFD solver, Ansys Fluent, was used for performing the CFD analysis for the current study. The default values for dynamic viscosity and density of water were taken from the Fluent's properties table (at standard temperature and pressure) and used for the calculation of Reynolds number.

Table 1: Simulation setup used for analysis

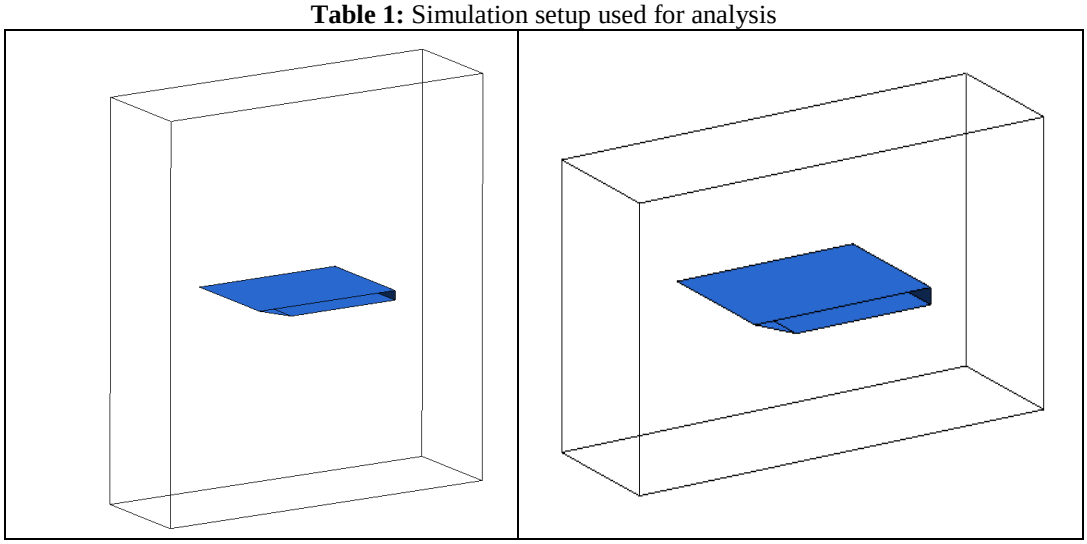

Validation Case	Baseline case
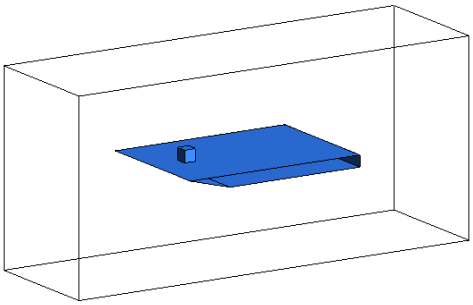	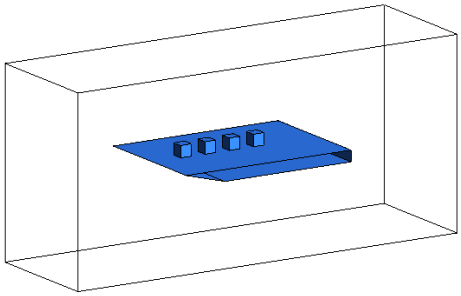
Case with 1 cube	Case with 1 row of cubes
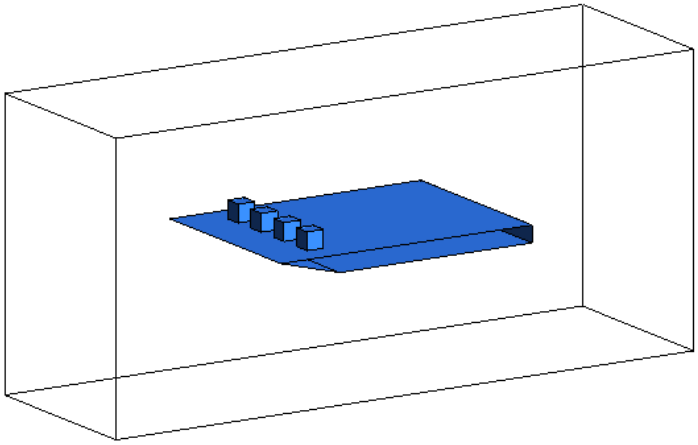	
Case with 1 column of cubes	

Based on the velocity and characteristic length (150 mm or 25.4mm) used in the experimental setup; the Reynolds number was either 907.64 or 151.67. Both the values of Reynolds number are in the laminar range. Hence for the current study, only laminar model was considered which improved the mesh generation cycle since parameters like y+ did not need to be considered as it did not affect the solution. Structured hexahedral mesh was generated for all the geometries and care was taken that the mesh obtained was of adequate quality. For the current study, it was ensured that the aspect ratio never exceeded 100 (the maximum aspect ratio recommended by Ansys Fluent).

No-slip wall condition was used to simulate the wall boundaries, with velocity inlet used as the inlet condition and pressure outlet used as the outlet condition. A velocity of 0.006 m/s was supplied at the inlet while the outlet was maintained at 1 bar pressure. For pressure-velocity coupling, SIMPLE algorithm was used with second order upwind scheme used for spatial discretization. A convergence criterion of 10^{-6} was used to confirm that the solution had fully converged with minimal possible error.

III. EMPIRICAL AND EXPERIMENTAL DRAG VALUE

Blasius [9] has derived an equation (as shown in Equation 1) for predicting the drag on flat plate for Reynolds number up to 10^6.

$$C_d = \frac{1.328}{\sqrt{Re_L}}$$

Equation 1: Blasius equation for drag coefficient over a flat plate for laminar flow

However, Janour [10] demonstrated experimentally that at lower Reynolds number of approximately 1000 or less, the Blasius analytical solution under-predicted the drag coefficient significantly. Since the Reynolds number (based on length L), Re_L used in the current study is in order of 900; the drag coefficient calculated using computational tool was compared to the drag data obtained from both analytical expression (Equation 1) and the experimental data. For the current study, the parameters used for the calculation of Re_L are shown in Table 2.

Table 2: Parameters used for calculation of Reynolds number

	Parameters	**Value**
U_∞	Free stream velocity	0.006 m/s
L	Length of flat plate	0.152 m
ρ	Density	998.2 kg/m^3
μ	Dynamic viscosity	0.001003 kg/m.s

Based on the above values, the Re_L was calculated using Equation 2, which yielded a value of 907.64.

$$Re_L = \frac{U_\infty * L * \rho}{\mu}$$

Equation 2: Equation for Reynolds Number

From the value of Re_L, the drag coefficient of 0.04408 was calculated using Equation 1. Based on experimental data, Janour [10] established an empirical correlation for the calculation of drag coefficient as shown in Equation 3.

$$C_d = 2.9 * Re_L^{-0.6}$$

Equation 3: Empirical correlation by Janour [10] for the calculation of drag coefficient

From the above equation, drag coefficient was calculated for the Re_L of 907.64 and was determined to be 0.04871. As it can be seen, Blasius equation under predicts the drag value by 9.5%.

IV. VALIDATION CASE WITH FLAT PLATE

For an initial validation of the simulated configuration, it was necessary that the wedged flat plate case be compared and validated against established results. Hence, a geometry specific for validation was generated with implicit understanding that the physics observed in the validation case study will be different from the baseline case. In order to validate the flat plate drag with the empirical and analytical data, a wedged flat plate was designed as fitted within a very large rectangular domain so that the effect of top and bottom walls was not felt by the flat plate. This was achieved by keeping the top and bottom walls 200 mm away from the flat plate surface as shown Figure 1. The mesh generated for the analysis is also shown in Figure 1.

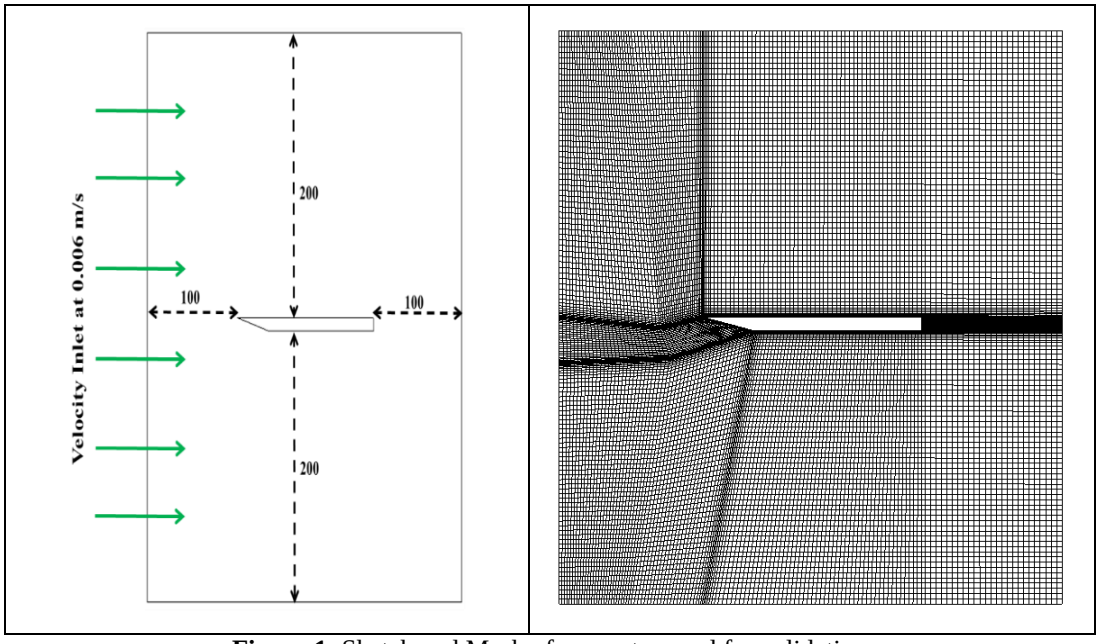

Figure 1: Sketch and Mesh of geometry used for validation

Initially, the side walls were modelled as translational periodic (cyclic) boundaries (as shown in Figure 2) so that no effects of the side surfaces would be felt on the flat plate. This was done to replicate the effective condition where flat plate is kept away from any surfaces that may produce hydrodynamic interaction.

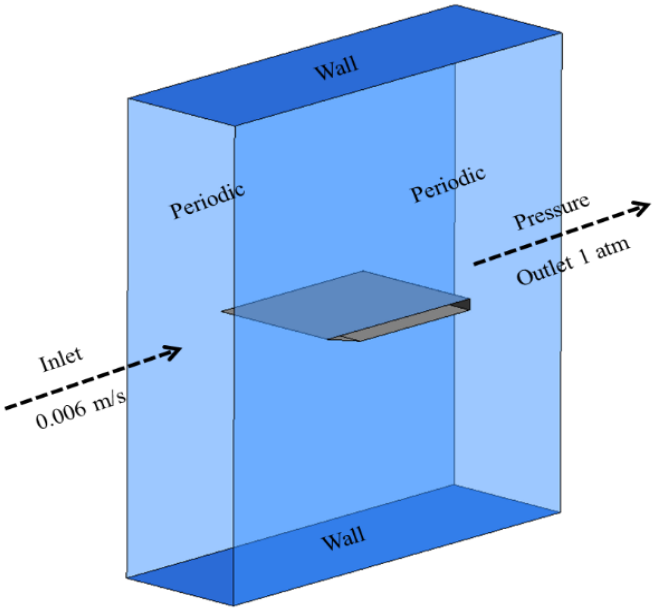

Figure 2: Schematic of boundary conditions used for validation case

It is understood that the baseline case will have side walls, and a corresponding interaction with the flat plate. Hence, as a further step; the side surfaces which were initially modelled as periodic conditions were later modelled as walls, to provide insight into the effect of wall viscous effects on the flat plate drag (as shown in Figure 3).

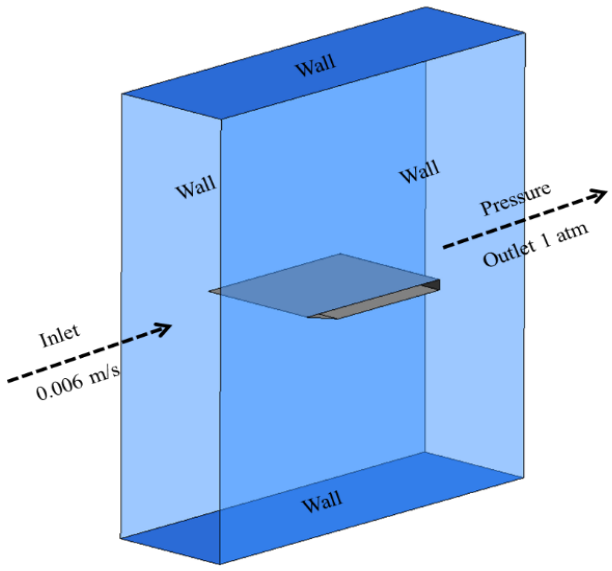

Figure 3: Schematic of boundary conditions used for case with walls

From the initial CFD analysis, the drag coefficient for the top surface of the flat plate was calculated for the validation case as 0.04875. This value was found to be 0.082 % higher than the value predicted by Janour's experimental data and 10.5% higher than the value predicted by Blasius's equation. Since it closely follows the value obtained from the empirical correlation given by Janour [10], it can be considered as the validation of the capability of computational tool to accurately predict drag values.

With the implementation of wall condition for side surfaces, it was observed that the drag value has further increased. This can be explained as the result of interaction of side wall boundary layer with flat plate boundary layer and accompanying losses. The drag coefficient predicted for this case was 0.05409, which was 10.95 %

more than the validation case value. Hence, the effect of side wall drag on the flat plate can be estimated to be 11%. This quantitatively defines the effect of perpendicular side walls on drag coefficient over a flat plate at low Reynolds number. The values from the study and corresponding difference from Janour's data is tabularized as shown below in Table 3.

Table 2: Summary of drag values from the validation cases and experimental data

Case	Drag Value	Difference from Janour's data	% Difference from Janour's data
Predicted by Blasius Equation	0.04408	0.00463	9.505
Predicted by Janour's experimental data	0.04871	-	-
Case with periodic side boundaries	0.04875	0.00004	0.082
Case with wall side boundaries	0.05409	0.00538	11.045

V. BASELINE CASE WITH FLAT PLATE

Once the basic validation study was completed, a flat plate configuration with boundaries similar to experimental conditions was analyzed. The previous validation study helped in isolating the effect of side walls on flat plate drag. The current study was instrumental in outlining the effect of distance of top and bottom walls on the drag prediction. It is understood that the top and bottom walls, when brought closer to flat plate would ideally "squeeze" the flow in between, thereby increasing the velocity between the flat plate and the walls. This would ideally increase the drag coefficient on the flat plate. The schematic, geometry and corresponding mesh generated is as shown in Figure 4, Figure 5 and Figure 6.

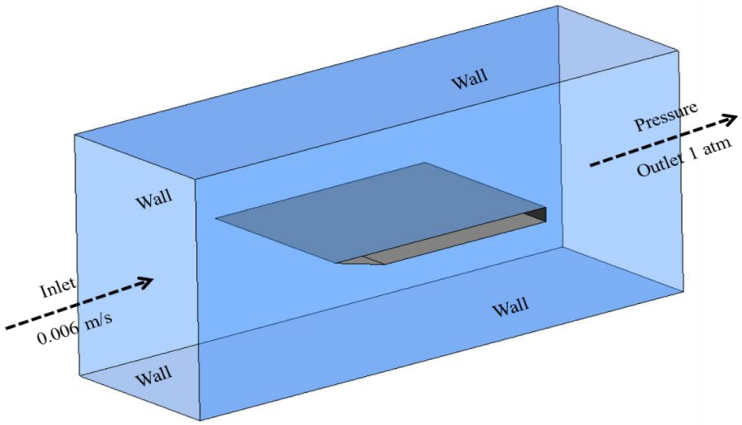

Figure 2: Schematic of baseline case

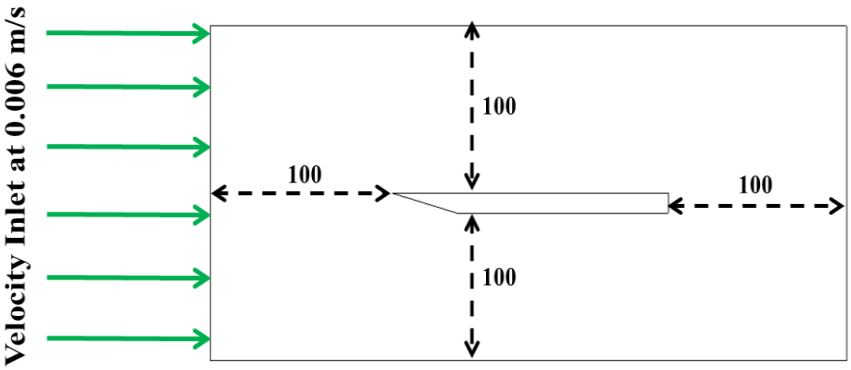

Figure 3 : Dimensions of computational setup used for baseline study

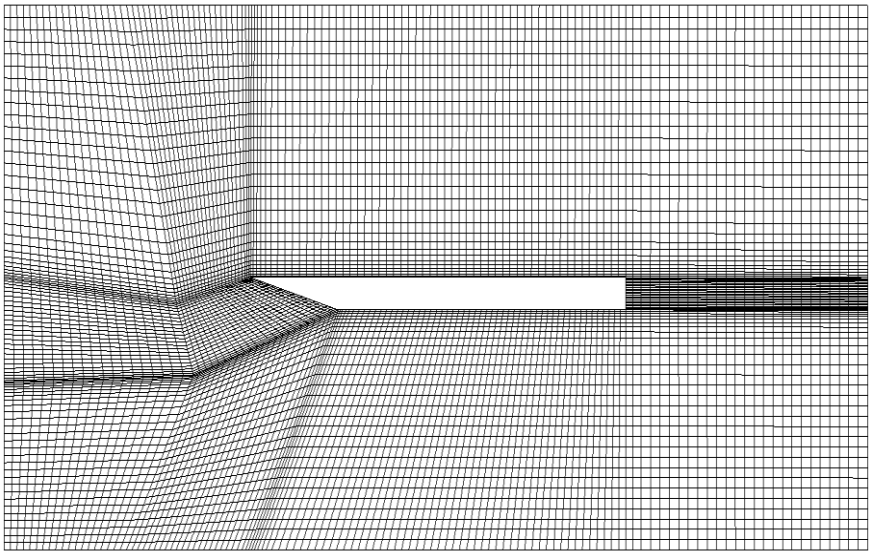

Figure 4: Mesh of geometry used as baseline flat plate model

For the baseline case with actual test condition dimensions, the calculated value of drag coefficient was 0.06273. This implies a drag coefficient increase of 16% (over the validation case with walls) when the top and bottom wall distances were reduced by half (from 200 mm to 100 mm) while maintaining all the other boundary conditions the same. The primary driver behind the increase in drag is the increase of viscous force on the flat plate due to the side wall boundary layer and increased velocity of the flow due to reduced area. From the contour plot of velocity shown in Figure 7, it can be observed that the velocity has increased up to 50% in some regions along the mid plane.

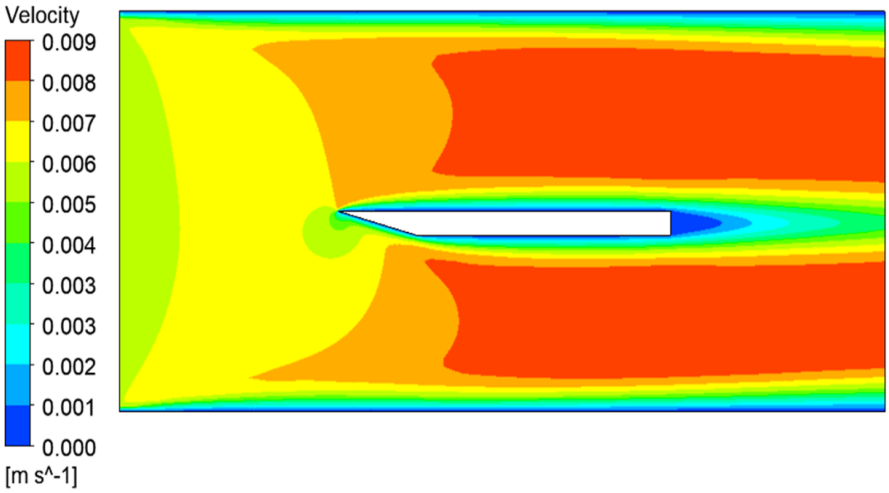

Figure 5: Contour of velocity profile along the midplane for baseline case

VI. CASE WITH SINGLE CUBE

Once the study with flat plate was completed, a single cubical protrusion of size 1000 mm^3 (10 mm x 10 mm x 10 mm) was added on the flat plate surface, at a distance of 25.4 mm (1 inch) from leading edge. This arrangement was also followed for experimental study to ensure that the leading-edge effect due to the flat plate does not interact with the stagnation zone formed in front of the protrusion. The local Reynolds number Re_x (based on the distance from leading edge) comes out to be 151.7, which makes the local flow condition laminar.

Since a systematic approach has been used to isolate the effect of side walls and top wall distance on the drag value over the flat plate, an addition of single protrusion and its corresponding rise in drag can be easily monitored. The geometry and mesh used for the study is as shown in Figure 8 and Figure 9. It can be seen from Figure 9 that zone near the cube is finely meshed so as to capture the flow physics near the cube more accurately.

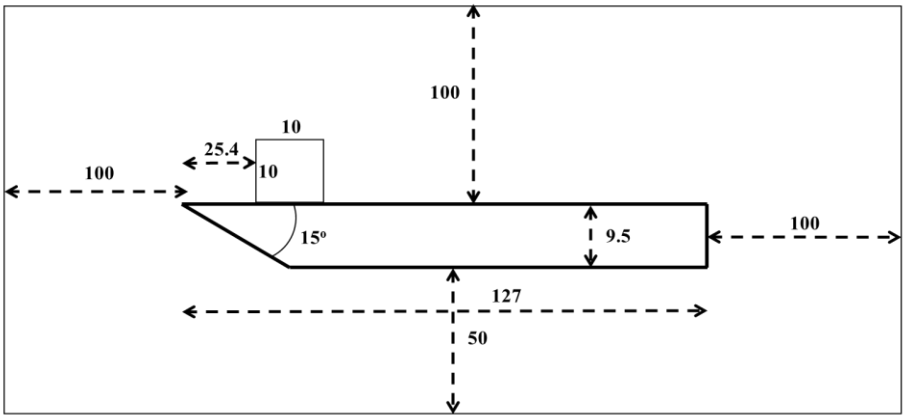

Figure 6: Dimensions of computational setup used for study with single cube (in mm)

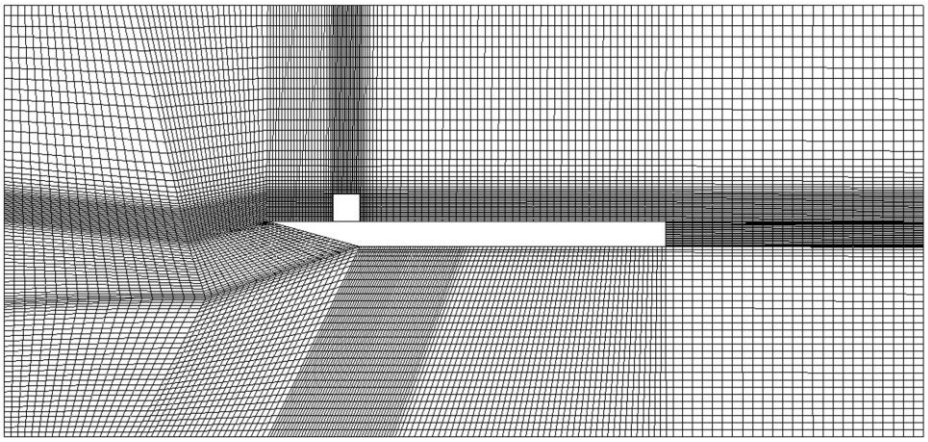

Figure 7: Mesh of geometry used for study with single cubical protrusion

From the computational study, it was determined that the drag coefficient was 0.06889 which is 9.8% higher than the case without any surface protrusion. The portion of drag coefficient rising from pressure component is close to 1% while from viscous component is close to 8.81%. It can be concluded that addition of one 100 mm^2 frontal area protrusion has led to nearly 10% increase in drag coefficient at low Reynolds number of 150. This value provides an indication of drag values caused by various surface protuberances on aerodynamically exposed surfaces. From the velocity contour along the midplane, we can establish that the flow is redirected by the cubical protrusion, which acts as a bluff body. The recirculation region behind the cube is referred to as a wake region with near zero velocity (as seen in Figure 10).

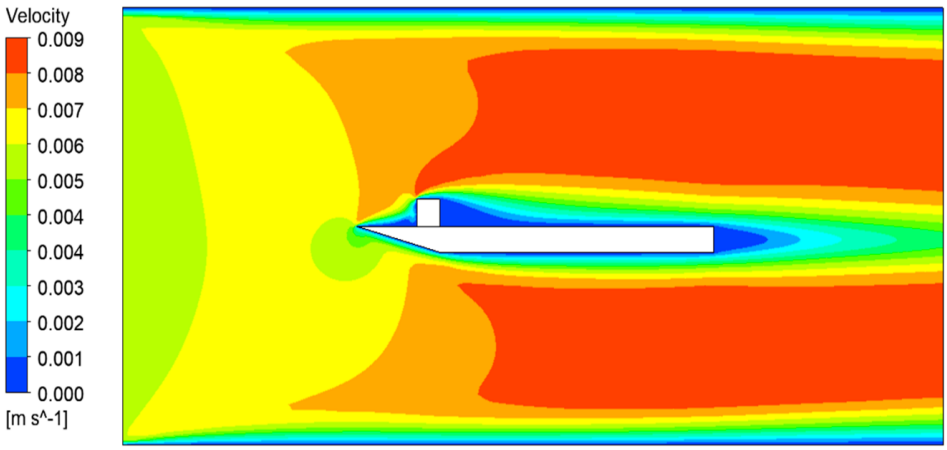

Figure 8: Contour of velocity profile along the midplane for case with single cube

VII. GRID SENSITIVITY STUDY

In order to ensure that all the computational studies conducted has been performed with an appropriate number of grid points, and that the analysis results have not been influenced by the number of grid nodes used; it is important to study and quantitatively establish the effect of grid points in attaining a solution. Initially a very small mesh was generated for the geometry which satisfies the minimum mesh quality requirements. This mesh is refined further by refining the cell size over each iteration. The results from all these meshes were compared, and the mesh size beyond which no significant change in target parameter occurs for any variation in mesh size was considered as the point of grid independence.

For the current study, four different meshes were generated starting from 0.32 million nodes. Once the solution from that case was obtained, the mesh was refined to obtain a higher quality mesh with increased mesh size of 0.56 million nodes. This process was continued twice more to obtain 2 more refined mesh. The result of grid sensitivity study is plotted as shown in Figure 11.

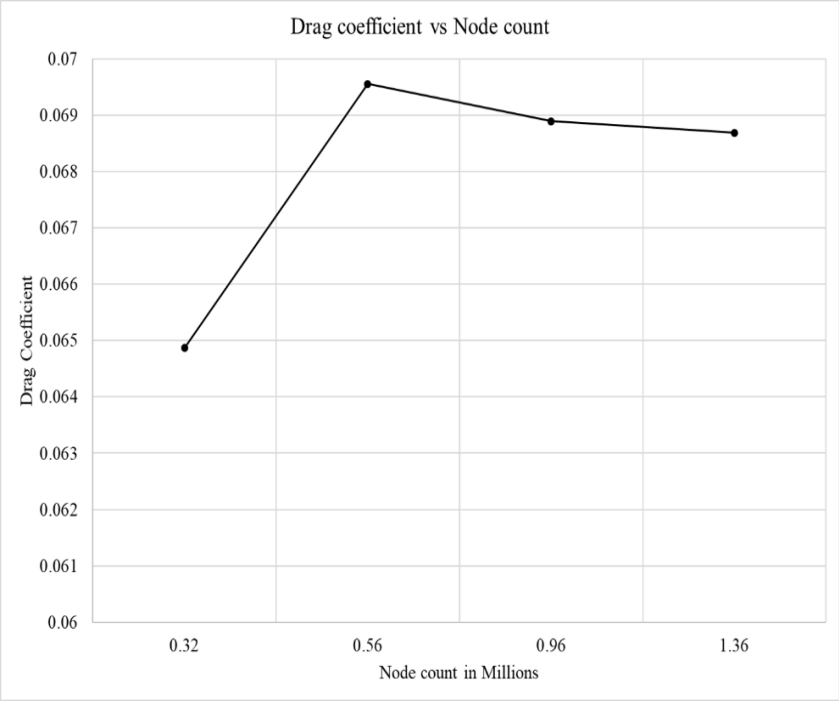

Figure 11: Grid Independence study based on drag coefficient

The data from the grid sensitivity study is tabulated as shown in Table 4. It can be observed that beyond the node count of 0.96 million nodes, the increase in node count did not produce significant change in the target parameter under study; in this case the drag coefficient. A 42% increase in node count beyond 0.96 million yielded only a difference of 0.29% in the drag coefficient value. Hence, 0.96 million was considered as the point where the solution became insensitive to the grid.

Table 3: Summary of grid sensitivity study

Mesh in Millions	Increase in mesh %	Drag Coefficient	% change in drag coefficient
0.32	-	0.06487	-
0.56	75.00	0.06955	7.21
0.96	71.43	0.06889	-0.95
1.36	41.67	0.068688	-0.29

VIII. CASE WITH SINGLE ROW AND SINGLE COLUMN OF CUBES

After establishing the drag value due to a single cube, the effect of four cubes were examined in two arrangements relative to the oncoming flow; in row formation and in column formation. It is to be noted that even though the number of cubes is same; the frontal area facing the flow is different based on configuration, which is expected to impact the drag parameters considerably. In the row formation, where all the cubes are in line with incoming velocity vector and with only one cube front facing the flow; the drag coefficient is expected to be lower, than when compared to that of column formation; where all the cubes are facing the flow. The configurations are as shown below in Figure 12 and Figure 13.

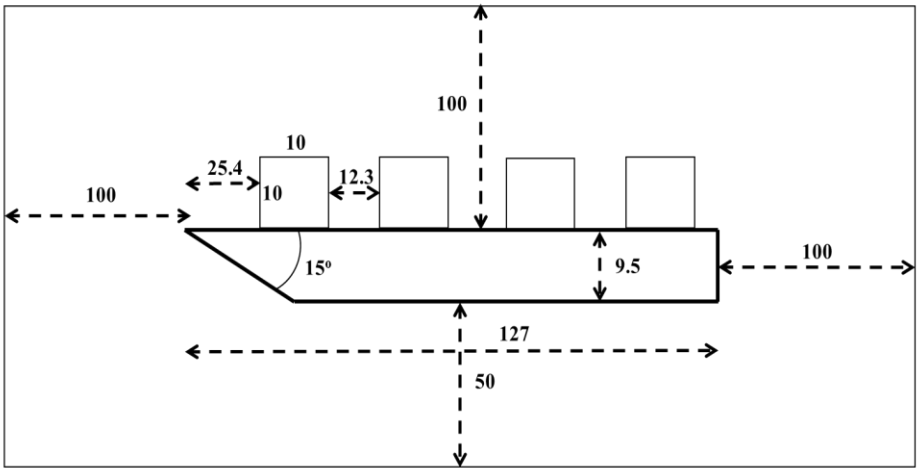

Figure 9*:* Dimensions of computational setup used for study with single row of cubes (side view)

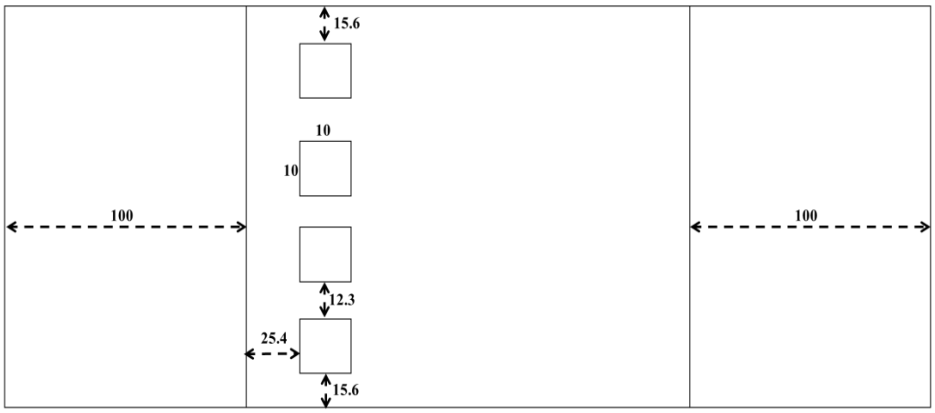

Figure 10: Dimensions of computational setup used for study with single column of cubes (top view)

Meshing strategy similar to single cube case was applied where the region near the cubes were meshed with fine mesh and region away from the cubes were fitted with coarser mesh to reduce computational resource usage. The mesh generated for the cases are as shown in the figures below. Figure 14 shows the side view of the mesh generated, while Figure 15 shows the top view of the mesh. The intricate refinement pattern in the mesh is used to ensure that all the physics relevant to the flow is accurately captured in the study.

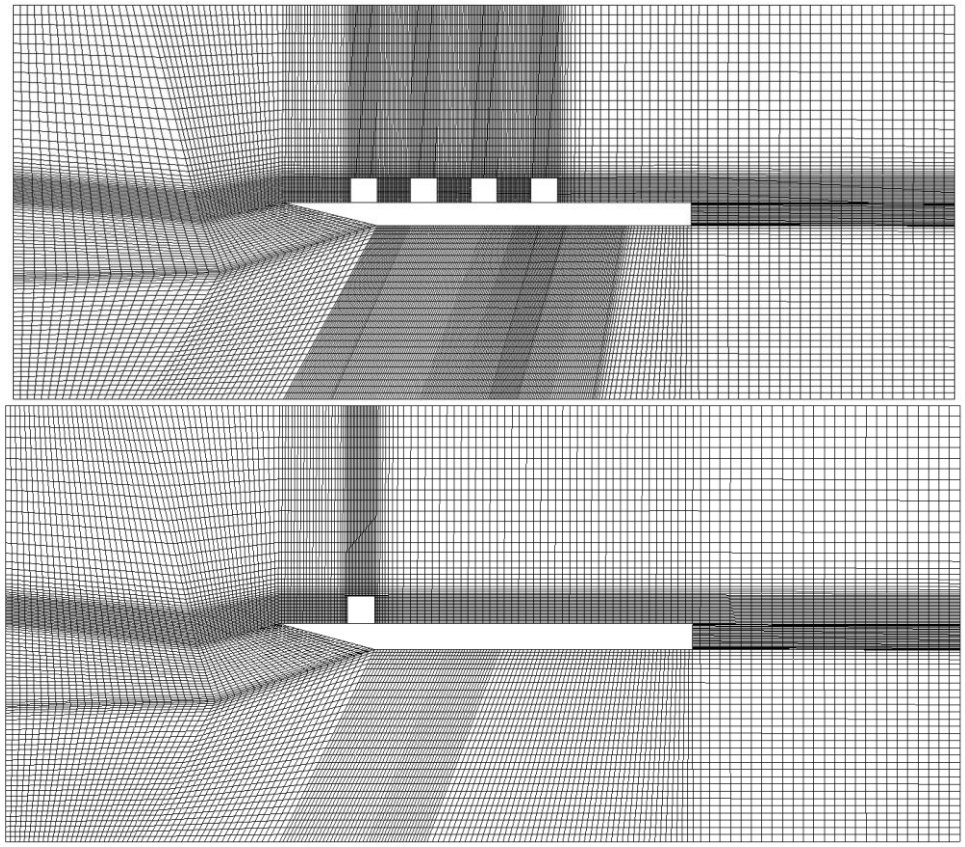

Figure 11 : Side view of mesh generated for the case study with single row and column of cubes

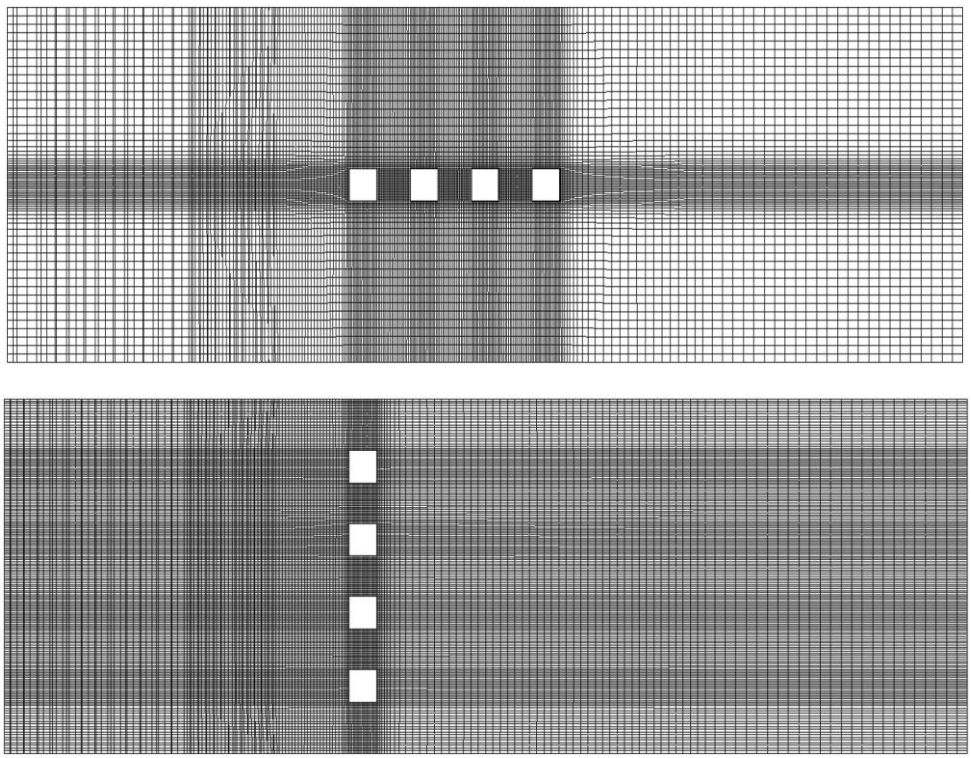

Figure 12: Top view of mesh generated for the case study with single row and column of cubes

The velocity contour along the mid-section through cubes is as shown in Figure 16 and Figure 17. Figure 16 shows the velocity profile along the side view of the geometry while Figure 17 shows the top view. It is important to note that in the row formation, the recirculation zone behind every cube is interacting with the

stagnation region formed in the front of the trailing cube. This interaction results in a reduced velocity approaching the cube and thereby reducing the drag effect.

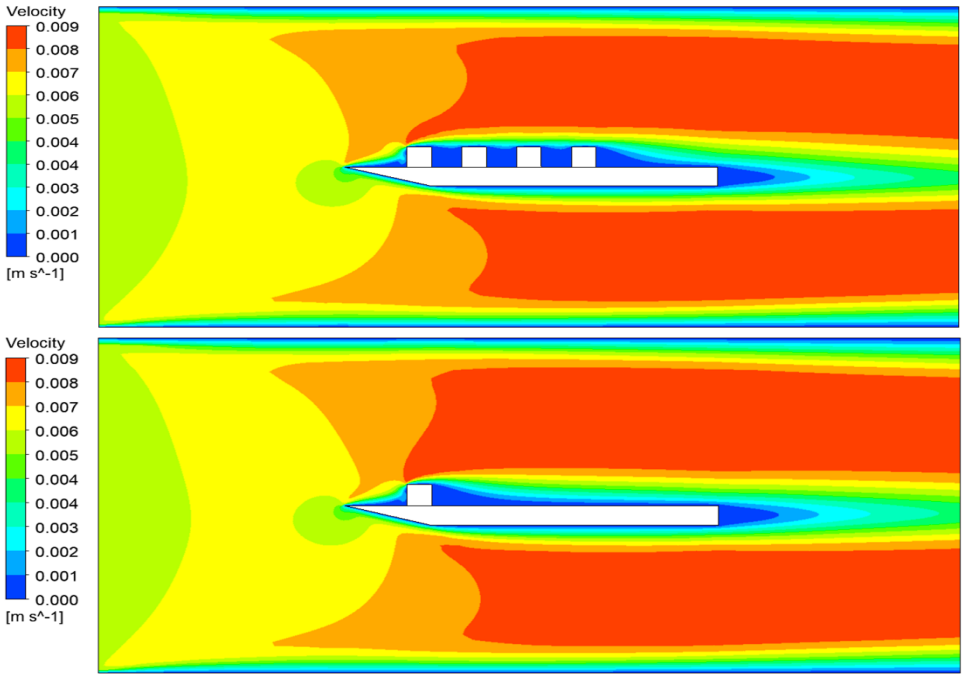

Figure 13: Side view of velocity profile for the cube study with single row and column of cubes

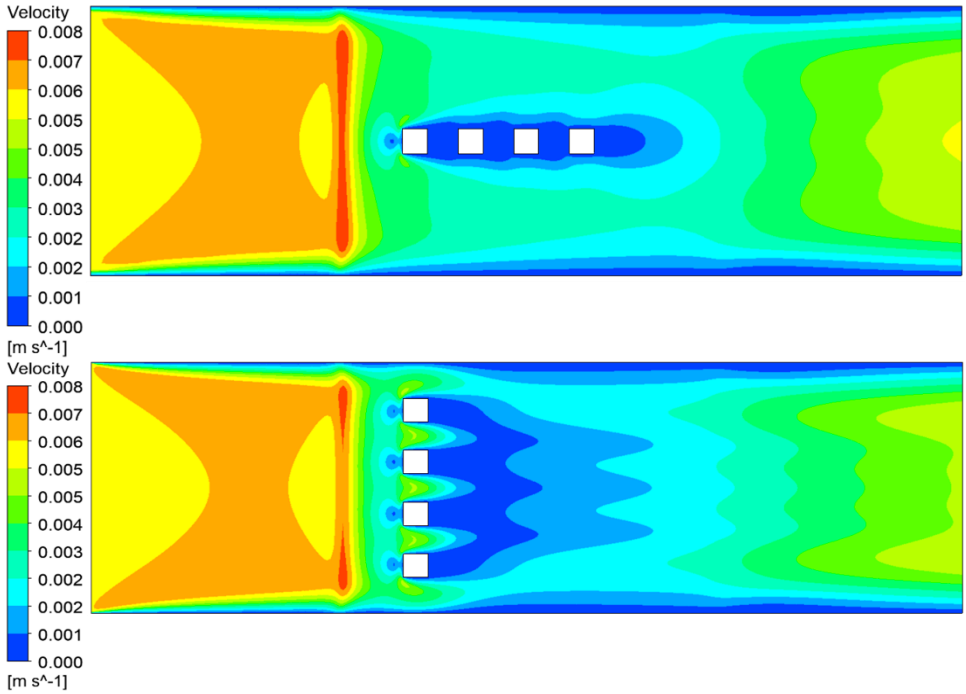

Figure 14: Top view of velocity profile for the cube study with single row and column of cubes

From the analysis, it was found that the drag coefficient for the case with four cubes in a row is 0.07395 which was 17.88% higher when compared to the case with no cubes. When compared to case with 1 cube, the addition of 3 more cubes in the row configuration increased the drag value by only 7.35%. This increase is significantly smaller than the increase seen by adding the cubes in column wise configuration.

When added in column-wise configuration, it was found that the drag coefficient has gone up to 0.8973 which was a 43.03% increase from the baseline study case, and 30.25 % increase from case with 1 cube. The almost proportional increase of drag coefficient when cubes are added in column-wise format (based on the result from

single cube case) is an indicator of validity of computational result in the given Reynolds number range. From the study, the complete data can be tabulated as shown in Table 5. The boundary conditions used for the sides walls and the domain height used are mentioned to help identify the effect of these parameters in the drag calculation.

Table 5: Summary of computational study

Description	Domain Conditions		Domain height above plate (mm)	Drag Coefficient on Flat plate	
	Side surface	Top surface		Total	% Increase from Baseline case
Validation case with periodic sides	Periodic	Wall	200	0.04875	-
Validation case with wall sides	Wall	Wall	200	0.05409	-
Baseline case	Wall	Wall	100	0.06273	-
Case with 1 Cube	Wall	Wall	100	0.06889	9.81
Case with 1 row Cube	Wall	Wall	100	0.07395	17.88
Case with 1 column Cube	Wall	Wall	100	0.08973	43.03

IX. SUMMARY

From the current study, it was established that domain conditions affect the flow properties like drag coefficient. Starting with validation setup; where initially the side surfaces were modelled as cyclic conditions; the drag coefficient on flat plate was 0.04875. When the side surfaces were later modelled as wall conditions, the drag coefficient increased to 0.05409; which is an approximate increase of 11%. This is the quantification of the effect of side-surface boundary layer on the flat plate drag. As the domain size is decreased to reflect the experimental test condition, it was noted that the drag coefficient on the top surface of flat plate further increases to 0.06273, which is an increase of 16% over the validation case with walls. This helped in sequentially identifying the effect of domain height in the calculation of drag parameter. The smaller setup thus obtained was treated as the baseline for further studies.

A single cube was then added 1 inch from the leading edge of flat plate to study the effect on drag based on presence of surface protrusion. Using the distance from the leading edge as length parameter, the local Reynolds number was calculated to be approximately 150. The drag coefficient was calculated from the computational analysis; and was found to be 0.06889. This 10% increase in drag can be attributed to the increase in pressure drag and viscous drag.

Further addition of 3 more elements, in row-wise configuration (ie along the flow direction) and in column-wise direction (ie across the flow direction) leads to drag values of 0.07395 and 0.08973 respectively; which is an increase of approximately 18% and 43% respectively from the baseline case. When compared to case with 1 cube, the addition of 3 more cubes in the row-wise configuration increased the drag value by only 7.35%; whereas addition in the column-wise configuration increased the drag value by only 30.25%. This study provided insight into the variation of drag values based on position of cubical surface protrusions and will act as stepping stone in further research conducted by the team where novel geometries will be used as surface protrusions. The result from current study is meant to act as validation model for the future cases.

Nomenclature

Acronyms

LES – Large Eddy Simulation
DES – Detached Eddy Simulation
RANS – Reynolds Averaged Navier-Stokes
CAD – Computer Aided Design
CFD - Computational Fluid Dynamics

Symbols

y^+ - Non-dimensional wall distance
C_d – Drag coefficient
Re_L – Reynolds number based on length L
U_∞ – Free stream velocity (m/s)
L – Distance from leading edge (characteristic length) (m)
ρ – Density (kg/m3)
μ – Dynamic Viscosity (kg/m.s)

REFERENCES

[1]. E. Meinders and K. Hanjalic, "Local convective heat transfer from an array of wall-mounted cubes," Int J. Heat Mass Transfer, vol. 41, no. 2, 1998.
[2]. E. Meinders and K. Hanjalic, "Experimental study of the convective heat transfer from in-line and staggered configuration of two wall-mounted cubes," International Journal of Heat and Mass Transfer, vol. 45, 2002.
[3]. E. Meinders and K. Hanjalic, "Vortex structure and heat transfer in turbulent flow over a wall-mounted matrix of cubes," International Journal of Heat and Fluid Flow, vol. 20, 1999.
[4]. H. Nakamura, T. Igarashi and T. Tsutsui, "Local Heat Transfer around a Wall-Mounted Cube in the Turbulent Boundary Layer," International Journal of Heat and Mass Transfer, vol. 44, no. 18, 2001.
[5]. H. Heidarzadeh, M. Farhadi and K. Sedighi, "Convective Heat Transfer over a Wall Mounted Cube Using Large Eddy Simulation," CFD Letters, vol. 4, no. 2, 2012.
[6]. S. Schmidt and F. Thiele, "Comparison of numerical methods applied to the flow over wall-mounted cubes," International Journal of Heat and Fluid Flow, vol. 23, 2002.
[7]. Y.-J. Hong, S.-S. Hsieh and H.-J. Shih, "Numerical Computation of Laminar Separation and Reattachment of Flow Over Surface Mounted Ribs," ASME, vol. 113, 1991.
[8]. M. Eslami, M. M. Tavakol and E. Goshtasbirad, "Laminar fluid flow around two wall-mounted cubes of arbitrary configuration," J. Mechanical Engineering Science, vol. 224, 2010.
[9]. H. Schlichting, Boundary-Layer Theory, 1951.
[10]. Z. Janour, "Resistance of a plate in parallel flow at low Reynolds numbers," NACA-TM-1316, 1951.

Raj Narayan Gopalakrishnan "Effect of Position of Wall Mounted Surface Protrusion in Drag Characteristics At Low Reynolds Number." IInternational Journal of Computational Engineering Research (IJCER), vol. 7, no. 11, 2017, pp. 26-39.